Steel converter slag as an oxygen carrier for chemical-looping gasification

Fuel Processing Technology 210 (2020) 106576

Contents lists available at ScienceDirect

Fuel Processing Technology

journal homepage: www.elsevier.com/locate/fuproc

Research article

Steel converter slag as an oxygen carrier for chemical-looping gasification

Fredrik Hildor[a,*], Henrik Leion[a], Carl Johan Linderholm[b], Tobias Mattisson[b]

[a] Chemistry and Chemical Engineering, Chalmers University of Technology, 412 93 Göteborg, Sweden
[b] Department of Space, Earth and Environment, Chalmers University of Technology, 412 96 Göteborg, Sweden

ARTICLE INFO

Keywords:
LD slag
Oxygen carrier
Chemical looping gasification
Steel converter slag
Water-splitting
Biomass

ABSTRACT

Chemical Looping Gasification (CLG) is a dual fluidized bed gasification technique where an oxygen carrier is used as bed material instead of sand. An optimized process could have several advantages, including i) one concentrated CO_2 stream, amiable for carbon capture, ii) less tar formation, iii) additional reaction pathways for syngas production, iv) less corrosion and v) CO_2 is generated in one stream from the fuel reactor that could be captured.

Steel converter slag, also called LD slag, is a by-product from the steel industry which, besides iron, contains significant fractions of Ca, Mg, Al and Mn in a complex matrix of phases. The low cost and presence of known catalytic solid phases in the slag makes it interesting as an oxygen carrier in CLG.

In this work, LD slag was investigated using a batch reactor with gaseous and solid fuel as well as with TGA. It was found that during gasification with LD slag, the material can i) transfer oxygen to the fuel, ii) catalyze the water-gas-shift reaction, iii) react with CO_2 forming carbonates and iv) split water to hydrogen. The overall result was a raw gas with a higher H_2/CO ratio for LD slag than the other tested materials.

1. Introduction

Gasification of solid carbon sources is one way to generate gaseous hydrocarbons (mainly CO, CH_4 and H_2) that can be used as gaseous fuels or for manufacturing of, e.g., liquid fuels or chemicals. During the last decades, the research field of biomass gasification has grown to a great extent due to the demand of renewable liquid and gaseous hydrocarbons [1,2]. Gasification of biomass is a favorable technology since it is flexible regarding feedstock and can be optimized for different outputs, and even using toxic feedstocks [3]. Gasification can be performed using different techniques where fluidized bed technologies have been widely used due to flexibility in fuel type and low emissions [4]. Fluidized beds can be used for indirect gasification at a larger scale using a Dual Fluidized Bed (DFB) gasifier system, producing a nitrogen-free product stream. Here a bed material, such as sand, is used to transport heat between the gasifier and combustor. By burning some of the fuel in the combustor, heat is generated and transferred to the bed material. This enables an auto-thermal process, albeit with some fuel conversion in the combustor with resulting carbon dioxide formation from the combuster, highly diluted in nitrogen [3,5].

The possibility to use different types of bed material could be a way for adjusting the outlet gas composition or provide oxygen to the fuel, as in Chemical Looping Gasification (CLG) [6]. CLG is similar to the Dual Fluidized Bed (DFB) gasification process, but with the difference that an oxygen carrier is used and no combustion occurs in the air reactor, see Fig. 1. Instead, full conversion of the char is -ideally- achieved with the presence of the oxygen carrier that provides oxygen to oxidize gasification inhibitors and a fraction of the gasified products [6–9]. CLG generates a syngas stream containing mainly H_2, CO and CO_2 that is obtained from the fuel reactor, see Fig. 1. Further, as is evident from Fig. 1, the exiting stream from the air reactor is free from carbon in CLG, in contrast to DFB gasification. This could have the advantage that corrosion issues from the air reactor/combustor are decreased, and the funneling of the carbon dioxide to the fuel reactor would mean that a higher fraction of carbon dioxide could be obtained in the same stream.

When using solid fuel such as biomass, it is of great importance that

Abbreviations: CLC, Chemical Looping Combustion; CLG, chemical looping gasification; DFB, dual fluidized bed; OCAC, Oxygen Carrier Aided Combustion; XRD, X-ray Diffraction; WGS, water-gas-shift; CO/C_t, Fraction of carbon monoxide to total carbon (CO, CO_2, CH_4); H_2/CO, Fraction of hydrogen to carbon monoxide; K_{eq}, Equilibrium constant for the water-gas-shift reaction; Q_i, The reaction quotient at the time *i*; n_i, Amount of substance *i* [mol]; m_i, Mass of substance i [g]; x_i, Fraction of substance *i* in gas [mol/m^3]; *P*, pressure [Pa]; *V*, volume [m^3]; *R*, Gas constant in ideal gas law; *T*, temperature [K] or [°C]; *t*, time [s]; *r*, char conversion rate as a function of time [(g/s)/g]; γ_{CO}, Conversion degree of CO; ω, Mass conversion on oxygen carrier, valued between 0 and 1; X_c, fraction of char conversion, a value between 0 and 1; $\dot{}$, Indicates a flow

* Corresponding author.
E-mail address: fredrik.hildor@chalmers.se (F. Hildor).

https://doi.org/10.1016/j.fuproc.2020.106576
Received 17 June 2020; Received in revised form 19 August 2020; Accepted 19 August 2020
Available online 30 August 2020

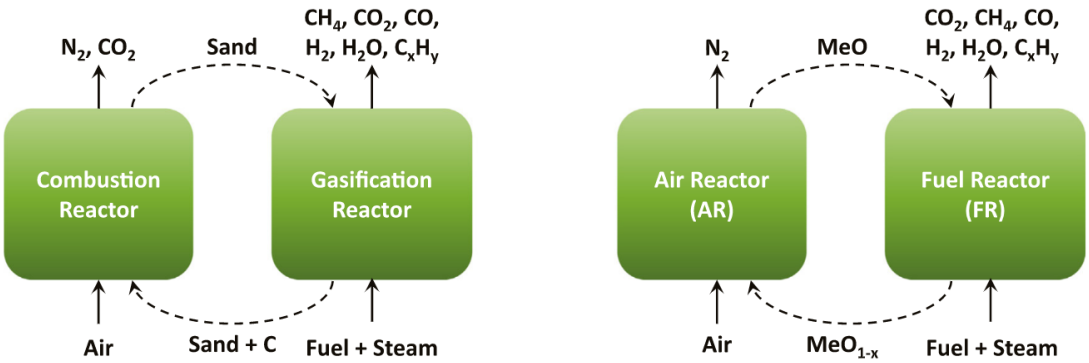

Fig. 1. Schematic overview of Dual Fluidized Bed (DFB) gasifier and Chemical Looping Gasification (CLG) and the role of the oxygen carrier.

the oxygen carrier is available at a low cost. Low-cost oxygen carriers are favored since the lifetime of the particles is decreased as a result of deactivation due to ash and losses when ash is separated from the bed material [10]. Low-cost oxygen carriers of iron have therefore been of interest since iron is highly available and can be sourced in large quantities [11,12]. Oxygen carriers of iron can be obtained from many different sources, including synthesized particles, ores or waste streams. The latter type of materials, waste streams that could be received at low cost from e.g. the steel industry, has been investigated previously with promising results [10,13,14].

In this study, LD slag was investigated as an oxygen carrier bed material for gasification. A laboratory batch fluidized bed reactor and a thermogravimetric analysis (TGA) was used to obtain a better understanding of the viability of this material and was compared to other bed materials: sand, olivine and ilmenite. Sand is the most commonly used bed material in conventional boiler techniques. Olivine is a non-oxygen-carrying active bed material used for gasification that reduces tar formation and agglomeration [15]. Ilmenite is a well studied iron-titanium ore oxygen carrier used in CLC and also evaluated in gasification [7,13]. However, all materials follow activation processes that may change some of the materials' chemical properties during gasification. Also addition of alkali or ash from the fuel itself may change the overall reactions [7,15–18].

LD slag (also called basic oxygen furnace slag or steel converter slag) is a by-product from the steel industry where pig iron from the blast furnace is converted into steel. Normally 85–165 kg LD slag is produced for every ton of produced steel [19], but the amount can be up to about 200 kg/ton steel [20]. LD slag contains mostly Ca and Fe with lower amounts of Mg, Mn, Si, Al and V. The transition metal content in this material allows LD slag to be utilized as an oxygen carrier. LD slag also has mechanical and chemical resistance that makes it possible to utilize it as a bed material for thermal fluidized bed fuel conversion techniques [21–23]. Since it is produced in large quantities and available due to limited demand, it is expected to be possible to obtain LD slag at similar or lower cost than sand [22].

LD slag contains various phases such as calcium-silicate-metal oxides, calcium oxide and metal oxides [24]. The main content of metals is iron, manganese and magnesium [21,24]. LD slag has been studied as an oxygen carrier in laboratory scale [21,25–28] and at semi-industrial scale [21,22]. These studies show that LD slag has a relatively low oxygen carrier capacity, ca 1 wt%. However, all studies so far are more related to CLC and not CLG, where the intention is to produce syngas and not fully convert the fuel to CO_2 and H_2O [6]. However, one of the components in LD slag, bimetallic calcium-iron oxygen carriers have been studied in CLG with promising results [29,30].

The gasification technology, although promising, needs to overcome many challenges to become viable. The most prominent issue is the formation of heavy condensable hydrocarbons, named tar, which condense at relatively high temperatures and can cause operational problems. In addition, biomass tar can correspond to 5–10% of the energy content of the fuel [7,31]. Conversion of tar is key to the efficiency of the process.

The potential advantages of CLG technology are numerous. In addition to the activity towards tar reforming, metal oxides ores can also promote the water gas shift (WGS) reaction. Besides, oxygen carriers are known to enhance char gasification [10]. A suggested explanation is that the concentration of inhibiting species around the char particles is lowered, due to the oxygen transported by the material. Volatile species, in particular tar and hydrogen, have been shown to inhibit char gasification [10,32–34].

However, the optimal operation of the chemical looping gasification process is complex. Partial combustion of the syngas may lead to a decrease in the energy content of the gas if oxygen transport can't be controlled, thereby decreasing the efficiency of the gasification process. For instance, Larsson et al. [7] investigated the impact of using ilmenite in the Chalmers' DFB gasifier to reduce the tar yield, with varying amounts of ilmenite diluted in silica sand, and reported a significant decrease in cold gas efficiency. Still, the fuel conversion should be complete in the fuel reactor of the CLG process, see Fig. 1. This means that a high CO_2 fraction will be generated in the fuel reactor in order to complete the heat balance for an auto-thermal process [6].

This study aims to investigate LD slag as bed material in a CLG process of biomass. By analyzing various parameters with respect to i) char gasification, ii) reaction of the oxygen carrier with important gaseous species and iii) catalytic reactions, the aim is to give an overall view of the propensity to use LD slag for CLG. The properties of LD slag are compared to other bed materials common in gasification in a laboratory fluidized bed operated both with solid and gaseous fuels.

1.1. Theoretical background

A solid fuel particle that is heated in a thermal conversion process will first dry to remove moisture. The dry fuel particle will after this pyrolyze resulting in volatiles with remaining solid char. This char particle will thereafter gasify to generate syngas [35]. During gasification of char using steam or CO_2, the main reactions are reaction (R1) and (R2), where C represents a solid fuel char for simplicity. The solid fuel is converted without the oxygen carrier being actively involved in the reaction mechanism. When including an oxygen carrier to the system, some of the released gasification products will be oxidized by the oxygen carrier to form H_2O and CO_2 according to reaction (R3) and (R4) [7,16]. MO_x in reaction (R3) and (R4) stands for a metal oxide that can be used as an oxygen carrier. Introducing an oxygen carrier can therefore partially convert hydrogen that is known to inhibit the char conversion [32,36]. Further, the reaction of H_2 and CO with the oxygen carrier will also increase the concentration of CO_2 and H_2O, which could enhance the gasification reactions.

$$C + H_2O \rightarrow CO + H_2 \quad \text{(R1)}$$

$$C + CO_2 \rightarrow 2CO \quad \text{(R2)}$$

Table 1
Elemental composition is given in wt% of the studied bed materials excluding oxygen.

Element	LD slag	Ilmenite	Olivine	Sand
Fe	17	36	5	0.36
Ti	0.78	28	–	0.04
Ca	32	0.22	–	0.05
Si	5.6	0.67	20	45
Mg	5.9	2.0	30	0.24
Mn	2.6	0.21	–	0.01
V	1.5	0.12	–	0
Al	0.76	0.17	0.24	0.22
Cr	0.33	0.06	0.21	0
Ni	0.002	0.03	0.25	0

$$MO_x + H_2 \rightarrow MO_{x-1} + H_2O \quad \text{(R3)}$$

$$MO_x + CO \rightarrow MO_{x-1} + CO_2 \quad \text{(R4)}$$

Clearly, there are many other reactions possible, including partial oxidation reactions to syngas by the oxygen carrier, in addition to a multitude of catalytic gas-phase reactions. It has been observed experimentally that the oxygen-carrying capacity of LD slag is mainly via the reduction of magnetite to wüstite [21]. This is somewhat surprising since the expected oxygen transport reaction for iron-based oxygen carriers is the reduction of hematite to magnetite [12]. This has been observed even in the presence of steam during the reduction phase [21]. Therefore, the formation of wüstite-like structures was expected for LD slag in these experiments, due to the low oxygen capacity. The formation of wüstite-structures provides the possibility for so-called water-spitting where wüstite is oxidized with steam to magnetite. Reaction (R5) [37] describes the water-splitting reaction that should be possible when significant steam fractions are available. Here, "A" indicates dopants such as e.g. Mg and Mn that are present in the crystal structure of the metal oxide regions in LD slag [21].

$$3Fe_{1-x}A_xO + H_2O \rightarrow Fe_{3-x}A_xO_4 + H_2 \quad \text{(R5)}$$

In addition to the reactions involving the oxygen carrier, there may also be important catalytic reactions which could be important for CLG. The most likely reaction is the water-gas-shift (WGS) reaction, given in R6. Having a bed material that catalyzes the WGS reaction is favorable for processes that aim to produce syngas with a high H_2/CO ratio or mainly H_2 [6].

$$CO + H_2O \leftrightarrow CO_2 + H_2 \quad \text{(R6)}$$

CaO is known to catalyze the WGS reaction described in reaction (R6) [38]. LD slag contains a high amount of calcium. However, calcium is present and bound into several different compounds such as calcium silicates and srebrodolskite, only a few percent is as free calcium. Free calcium in this context means in the form of CaO and Ca$(OH)_2$ as well as $CaCO_3$ that is remaining's of the lime added in the Linz–Donawitz steel converter process [24]. In this specific batch of LD slag, the amount of free calcium has been measured to roughly 4 wt% for heat-treated samples [21]. The presence of free calcium might be favorable for the use of LD slag in a CLG process since it may catalyze the WGS reaction.

In relation to this, the presence of free calcium and $CaCO_3$ may affect a chemical looping process since it may form carbonates in the fuel reactor, see R7. This could affect the gas-phase in the fuel reactor, by shifting reaction (R6) towards the right, i.e. promoting hydrogen production. Still, this would mean that there would be a transport of carbon over to the air reactor. In the air reactor, carbonates can be decomposed to form CaO according to the reverser of reaction (R7). The forward reaction in (R7) will in this paper be referred to as carbonation and the backward reaction referred to calcination.

$$CaO + CO_2 \leftrightarrow CaCO_3 \quad \text{(R7)}$$

These three reactions; 1) water-splitting, 2) catalytic towards WGS and 3) carbonation, that is bound into the material of LD slag may affect the usage of LD slag as an oxygen carrier. These properties may be of interest both regarding CLC and CLG and therefore need to be further investigated. This work investigates these potential reactions for LD slag and if these will affect a gasification process. LD slag is used in a detailed experiment using a fluidized batch reactor at a laboratory scale and compared to other bed materials.

2. Material and methods

Two oxygen carriers, LD slag and ilmenite, were investigated in this work and compared to sand and olivine. Ilmenite is a bench-mark oxygen carrier and used here as reference material. Both LD slag and ilmenite have been tested as oxygen carriers for Oxygen Carrier Aided Combustion (OCAC) in large scale as well as smaller scale for CLC [21,22,39,40] and CLG [7]. LD slag was received from SSAB in Sweden. The particles were sieved to 150–400 μm. Rock ilmenite was received from Titania in Norway and sieved to 100–300 μm. These materials were heat-treated for 24 h at 950 °C in air before laboratory fluidized bed experiments. The small deviation in particle size is not expected to have a major impact on reactivity. The elemental composition of these materials can be seen in Table 1.

The two oxygen carriers were compared to two non-oxygen carrier materials; sand and olivine. Olivine was provided by Sibelco Nordic AB and hade a size distribution of 180–500 μm. The elemental composition of the olivine can be seen in Table 1 [15]. The olivine was heat-treated at 950 °C for 24 h in the same manner as the oxygen carriers. The sand used had a size range of 180–250 μm and was extra pure sea sand provided from Merck.

The wood pellet for the batch fluidized bed experiments was devolatilized at 820 °C under nitrogen atmosphere in a silica sand fluidized bed. The silica sand was then separated from the devolatilized pellets by sieving. The devolatilized pellets were then crushed and sieved to extract the desired size range of 180–300 μm for the laboratory fluidized bed. The volatiles content in the pellets was determined to roughly 82 wt% on dry basis. Analyses and fuel properties can be seen in Table 2.

The lower heating value (LHV) of the pellets was roughly 18.9 MJ/kg on dry basis. For the pellets char, the LHV was determined to 32.6 MJ/kg on a dry basis.

2.1. Laboratory fluidized bed reactor

The laboratory fluidized bed batch reactor was constructed of quartz glass with an inner diameter of 22 mm with a porous plate

Table 2
Fuel analysis of the pellets and devolatilized pellets used in the experiments. Samples are converted into ash at 550 °C in an inert atmosphere. Values are given in wt %.

	Dry basis					On ash samples							
	Ash	S	C	H	O	Fe	Ca	Mg	Mn	Al	K	P	Si
Pellets sample	0.4	< 0.02	50.3	6.2	43	0.89	22	3.6	2.7	1.1	9.6	1.4	4.0
Pellets char sample	3.5	0.02	93.5	< 0.5	3	3.9	21	4.8	2.9	1.5	5.8	1.3	6.6

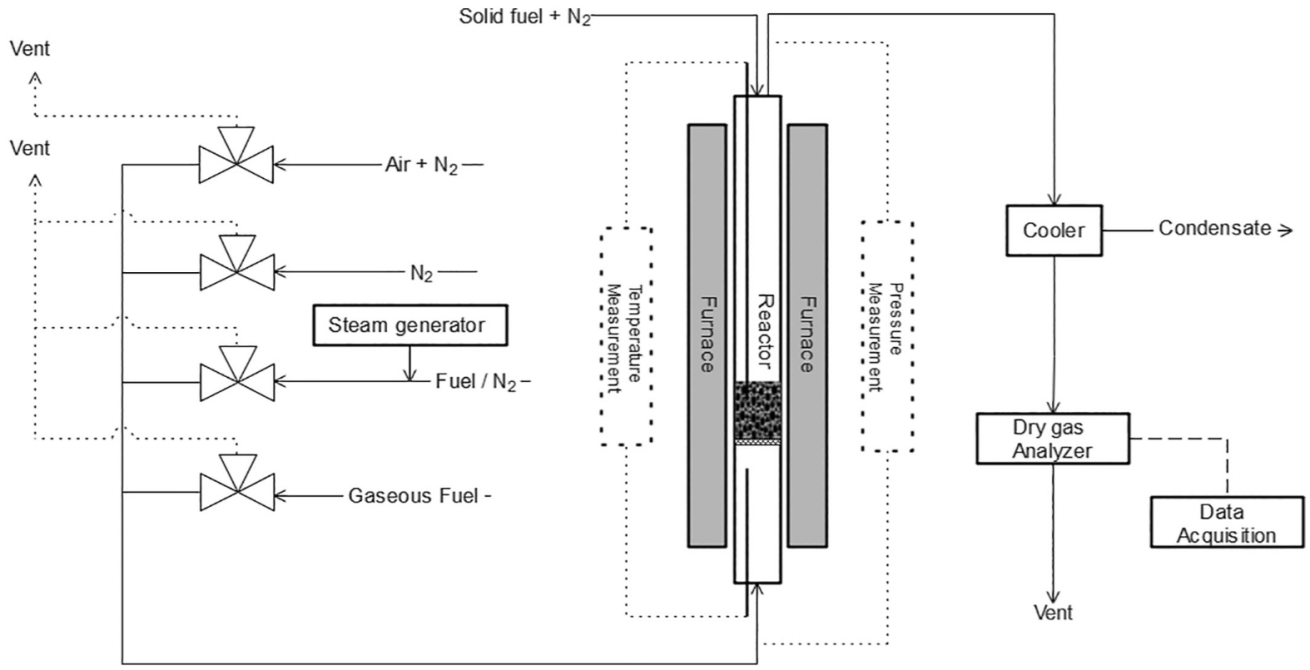

Fig. 2. Schematic layout over the batch reactor used for gasification experiments.

placed 370 mm from the bottom where particles were placed. The reactor was mounted inside an electrically heated furnace and was equipped with a pressure sensor (Honeywell pressure transducer 20 Hz) to monitor pressure fluctuations over the reactor. Two K-type thermocouples enclosed in quartz glass, one mounted in the bed and one mounted under the porous plate, were used to determine the temperature in the bed. A schematic overview of the batch reactor can be seen in Fig. 2. Tubing was electrically heated to prevent condensation of steam to water. Steam was generated from a CEM-system (Controlled Evaporation Mixing) and gasses were mixed prior to the reactor.

To determine the dry-gas concentrations from the laboratory fluidized bed, the gases from the reactor were cooled and water condensed, then the gases were analyzed using a Rosemount NGA 2000 analyzing CO, CO_2, CH_4, H_2 and O_2. The frequency of gas composition measurements was 1 Hz. A detailed overview of the laboratory system is presented elsewhere [41].

Prior to all experiments in the laboratory fluidized bed reactor, activation of the bed material was performed. Particles were first heated up to 850 °C in oxidizing conditions containing N_2 with an O_2 content of 5%, using a total flow of 1000 ml/min. This flow corresponds to roughly four times the minimum fluidization velocity for particles with a mean size of 250 μm and a density similar to sand. The bed material was then activated by alternating oxidizing and reducing conditions with intermediate inert flushes using N_2. The reduction during activation cycles was performed with the addition of syngas (50% CO in H_2) with a flow of 900 ml/min. The particles were cycled with syngas until the reactivity with syngas was constant, between 10 and 25 cycles for the different materials. The reason for this procedure is to make sure that any initial recrystallization or phase changes will be completed before the solid fuel experiments begin.

2.1.1. Gasification experiments

For the solid fuel experiments in the laboratory fluidized bed batch reactor, a sample of 40 g of bed material was used. Following the syngas activation, the sample was first oxidized with 5% O_2, which was followed by a short flush with nitrogen. After this period, devolatilized wood pellets were inserted from the top of the reactor in a stream of 500 ml/min N_2. Normally, 0.2 g of devolatilized pellets char in the size range of 180–320 μm was used. However, fuel amounts up to 0.6 g was used to reduce the bed further for some tests. During solid fuel periods, the bed material was fluidized using 50% steam in N_2 with a flow of 1000 Nml/min at a furnace temperature ranging from 820 °C to 970 °C. This oxidation-inert-reducing-inert series, or cycle, was then repeated three times at each temperature and results were averaged for all three cycles in the evaluation. Fig. 3 shows one typical cycle of solid fuel gasification with LD slag at 970 °C. When the oxygen is replaced with inert gas at (time = 0 s) the oxygen concentration rapidly drops as the oxygen is flushed from the system. The solid fuel is introduced at 180 s, and the gasification proceeds, as indicative by the rising concentrations of CO_2, CO and H_2. It is clear that the reaction towards CO and CO_2 is higher during the initial parts of the reduction and then decreases. The same behavior is not seen with H_2 which increases at the same time as the concentration of C-species decrease. In fact, there is H_2 out from the reactor even when all char is converted, which indicates that steam is

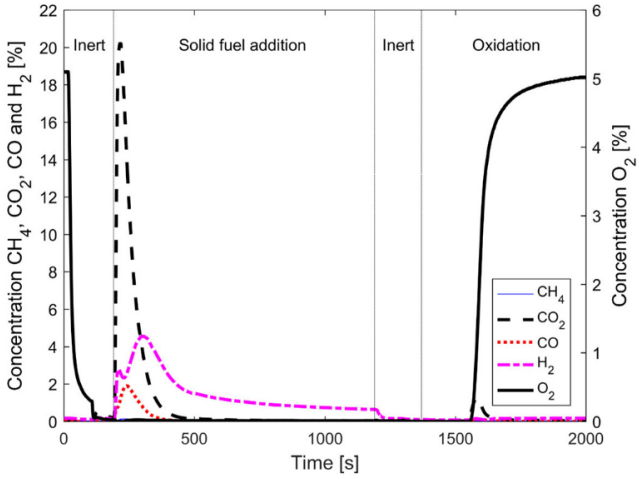

Fig. 3. One cycle at 970 °C of char gasification using LD slag as bed material in the laboratory scale fluidized bed.

generating H_2 by water spitting. During the oxidation period, oxygen is first fully reacting with the particles, clearly seen as no gas-phase O_2 exits from the reactor initially. At about 1600 s the oxygen increases as the oxygen carriers are becoming saturated with oxygen. At the same time as gas-phase O_2 is released a small amount of CO_2 is released. This CO_2 originates from the combustion of unconverted char and char that was trapped on the walls of the upper part of the reactor tube.

2.1.1.1. Data evaluation. For the solid fuel experiments, it is important to evaluate both the char reactivity as well as the gas conversion and selectivity. The total molar gas yield for each component from the gasification of the char for a cycle, or a part of a cycle, was calculated with Eq. (E1) between time t_1 to time t_2. The total molar flow was calculated using Eq. (E2). Assumptions are that the only outgoing gases of significant volume in the non-condensed gas are CO_2, CO, H_2 and CH_4.

$$n_{i,t} = \int_{t_1}^{t_2} x_{i,out} * \dot{n}_{out}\, dt \tag{E1}$$

$$\dot{n}_{out} = \frac{P}{RT} * \frac{\dot{V}_{N_2,in}}{1 - (x_{CO_2} + x_{CO} + x_{H_2} + x_{CH_4})} \tag{E2}$$

The fraction of char conversion, X_c, is defined as the cumulative carbon released at a certain time divided by the total carbon emitted from the converted char during the reduction period. These are defined as in Eqs. (E3) and (E4). The integral in Eq. (E4) is evaluated on the data from char insertion ($t_1 = t_{red,\ start}$) until the end of the reduction when the atmosphere is changed to inert ($t_2 = t_{red,\ end}$).

$$X_c(t) = \frac{m_c(t)}{m_{c,tot}} \tag{E3}$$

$$m_c(t) = M_c \int_{t_1}^{t_2} \dot{n}_{out}(t)(x_{CO}(t) + x_{CO_2}(t) + x_{CH_4}(t))dt \tag{E4}$$

The gasification rate (r_w) was calculated using Eq. (E5) where $\dot{m}_c$ was the mass-based rate of conversion of carbon. The gasification rate was then normalized using Eq. (E6). In this work, a mean value for the gasification rate was normally extracted from the gasification rate between a char conversion of $0.3 < X_c < 0.7$, as has been done in earlier studies [42]. The reason for this conversion span is that the gasification rate is more stable in this region and easier to compare to other experiments.

$$r_w = \frac{dX_c}{dt} = \frac{\dot{m}_c}{m_{total}} \tag{E5}$$

$$r = \frac{r_w}{1 - X_c} \tag{E6}$$

In addition to the char conversion, the gas phase conversion is also very important. Two parameters have been used in this work in order to evaluate the gas conversion: i) the conversion of carbon species to CO and ii) the H_2/CO molar ratio. The former is defined as Eq. (E7). Here the molar yield of each component is calculated using Eq. (E1) between $0.3 < X_c < 0.7$.

$$\frac{CO}{C_t} = \frac{n_{CO}}{n_{CO} + n_{CO_2} + n_{CH_4}} \tag{E7}$$

Re-oxidation after the reduction cycle, correlated to the omega value at the end of the cycle, was calculated using Eq. (E8). A reference O_2 curve using inert sand in the same experimental conditions was used to determine the point of transition between inert and oxidizing conditions. The difference between the actual uptake using an oxygen carrier and the reference cycle with inert is then judged to be a result of O_2 uptake of the oxygen carrier.

$$O_{2,re-oxidation} = \int_{t_{ox}=0}^{t_{ox}=end} (x_{O_2,ref} - x_{O_2,sample}) * \dot{n}_{out} \tag{E8}$$

Since there are both traces of soot and some remaining char, the final O_2 consumed by the oxygen carrier is calculated by subtracting the molar CO_2 generated during oxidation from the total O_2 uptake during the same period.

The equilibrium constant K_{eq} for the WGS reaction (R6) is defined as in Eq. (E9) when gases are at equilibrium. The temperature dependence of the equilibrium at atmospheric pressure is shown in the same equation [43,44]. The reaction quotient Q_i is defined similarly as the equilibrium and calculated for the outgoing gases from the reactor at the time *i*, see Eq. (E10). Q_i is used to estimate how far the concentrations of the gases are from the equilibrium. If $Q_i = K_{eq}$, the gases are at equilibrium with respect to reaction (R6).

$$K_{eq} = \frac{x_{CO_2} * x_{H_2}}{x_{CO} * x_{H_2O}} = \exp\left(-4.33 + \frac{4577.8}{T}\right) \tag{E9}$$

$$Q_i = \frac{x_{CO_2,i} * x_{H_2,i}}{x_{CO,i} * x_{H_2O,i}} \tag{E10}$$

In the equations above, x is the outgoing fraction of gas species.

2.1.2. Gaseous fuel experiments

A series of experiments were done with gaseous fuel in order to better elucidate the reaction mechanisms of the oxygen carrier. The same experimental setup as described in Section 2.1 was used to determine the reactivity with CO and syngas at different oxidation levels and temperatures. Here, the fuel was introduced from the bottom of the reactor. The bed material used was 5 g LD slag or ilmenite mixed with 10 g sand. Mixing an oxygen carrier with an inert material such as sand in this particular experimental setup is a common procedure. This to obtain a viable fluidized bed when using a relatively small amount of bed material necessary in order to avoid full conversion of inlet gases [41]. The temperature was varied between 670 °C and 970 °C with 50 °C steps. At each temperature, three cycles were performed. Inlet gases for these experiments were either 900 ml_N/min 50% CO in H_2, referred to as syngas, or 900 ml_N/min 50% CO in N_2 during a 20 s reduction for every cycle. Oxidation was performed with 1000 ml_N/min 5% O_2 in N_2 until full oxidation and intermediate inert flushes were performed with 1000 ml_N/min N_2 for 180 s.

2.1.2.1. Data evaluation. CO conversion (γ_{CO}) from the conversion of CO or syngas is defined according to Eq. (E11) in this paper.

$$\gamma_{CO} = \frac{x_{CO_2}}{x_{CO_2} + x_{CO}} \tag{E11}$$

The mass-based conversion of the oxygen carrier (ω) represents the degree of oxidation of the oxygen carrier and can be calculated from Eq. (E10) below, where $\omega = 1$ corresponds to the fully oxidized oxygen carrier. m_{ox} is defined as the oxidized mass of the oxygen carrier and *m* is the actual mass. Calculating the ω at time t_i during reduction was done using Eq. (E13) for syngas [45] and Eq. (E14) for CO.

$$\omega = \frac{m}{m_{ox}} \tag{E12}$$

$$\omega_{t_i} = \omega_0 - \int_{t_0}^{t_i} \frac{\dot{n}_{out} M_O}{m_{ox}} (2x_{CO_2} + x_{CO} - x_{H_2}) \tag{E13}$$

$$\omega_{t_i} = \omega_0 - \int_{t_0}^{t_i} \frac{\dot{n}_{out} M_O}{m_{ox}} (x_{CO_2}) \tag{E14}$$

2.1.3. Water splitting

From Fig. 3 it is apparent that water-splitting of steam to H_2 is a possible mechanism. For the experiments used to test the extent of water-splitting for the LD slag, the experimental setup described in Section 2.1 was utilized. Here a bed of 5 g of LD slag mixed with 10 g of sand was used. The reduction of the LD slag was performed with 50% CO in N_2 during a 20 s reduction for every cycle. After reduction, the particles were flushed with 1000 ml_N/min N_2 followed an oxidation

50% H_2O in N_2 with a flow of 900 ml_N/min. The experiment was conducted until the H_2 concentration in the outlet was below 0.01%. Another N_2 flush and then final oxidation using O_2 was performed with 1000 ml_N/min 5%O_2 in N_2 until full oxidation of the particles. These cycles were performed at 870C.

2.1.3.1. Data evaluation. Calculations of the generated flow of H_2 production for these experiments were calculated using Eqs. (E1)–(E2). The following oxygen uptake during oxidation using 5% O_2, was calculated with Eq. (E8).

2.1.4. Calcination/carbonation experiments

The fact that the LD slag has a significant fraction of CaO, makes reaction with CO_2 forming $CaCO_3$ possible. In order to investigated this further, calcination and carbonation, i.e. reaction (R7) of LD slag were studied. This was done using a thermogravimetric analyzer (TGA) from TA Instruments model Q500. A 25 mg sample of heat-treated LD slag was used in a ceramic crucible and heated up to 950 °C under oxidizing conditions, 5% O_2 in N_2. This was the same for both calcination and carbonation experiments.

For calcination experiments, the temperature was decreased to 850 °C at which point the atmosphere was changed to 100% CO_2 to fully carbonate the sample. When full carbonation was obtained, i.e. no additional weight gain was noted, the temperature was decreased to 650 °C with a cooling rate of 5 °C/min, then the atmosphere was changed to diluted CO_2 in nitrogen to a concentration between 10 and 100% CO_2. When the desired CO_2 concentration was set, the temperature was ramped with 10 °C/min until 950 °C and the temperature where calcination started, i.e. weight decreased due to loss of CO_2, was noted. Thereafter the temperature was decreased to 850 °C and the sample carbonated again to repeat the calcination at another CO_2 concentration.

For carbonation experiments, the heat-up procedure was similar to the calcination experiments. After the oxidation at 950 °C, however, the air was switched to CO_2 concentration between 10 and 100%, after which the temperature ramped down with 5 °C/min until 650 °C was reached. The temperature where the weight of the sample started to increase due to carbonation was noted and used for the evaluation. Thereafter the temperature was increased to calcine the particles and a new CO_2 concentration set and the experiment repeated.

3. Results

3.1. Solid fuel conversion

Fig. 4 shows the concentration profiles of outgoing gases for all four investigated materials at 870 °C. It is clear that, after fuel addition, there is an initial higher concentration of CO_2 for the experiments with oxygen carriers compared to olivine and sand. This is expected, as the oxygen carrier will react with gasification products forming CO_2. Further, the H_2 profiles are also different with respect to the oxygen carriers and the "inert" particles. The latter materials both have a significant fraction of H_2 initially, which decreases as a function of time, and virtually no H_2 after the carbon is converted. For LD slag the H_2 concentration is initially low, but increases as the CO_2 decreases, and in fact, decreases very slowly, with some H_2 present even when all carbon is converted. For ilmenite, the H_2 peaks early, and then decreases similarly to the sand and olivine samples. It can be observed that the CH_4 production in all cases is negligible compared to CO, CO_2 and H_2.

To investigate how much of the char was lost in the gas flow and not converted in the reactor, a cold set up with a filter was tested. Here it was concluded that up to 5% of the char was lost as fines using a flow of 5000 ml_N/min, which corresponds to 120% of the expected gas velocity inside the reactor at 970 °C. However, some char may also be lost as partly gasified char particles, which decrease in size and density during the reaction, which may result in lower terminal velocity of the particles and hence elutriation. Still, it should be noted that although there is likely some char that bypassed the reaction zone, the evaluations of char conversion are based on the converted char only.

3.1.1. Char conversion

Fig. 5 shows the instantaneous gasification rate r as a function of X_c, as defined in Eqs. (E3)–(E4). The outgoing gases are also included for comparison. Evidently, the LD slag has a somewhat different gasification pattern compared to the other bed materials. For the other materials the rate *r* is constantly increasing over X_c, but for LD slag the rate levels out and start to decrease at roughly $X_c = 0.4$. This point is in conjunction with an increase in H_2 concentration. The shape of the curves for LD slag does suggest that water splitting is occurring. When the bed material is reduced, H_2 is formed following reaction (R5). The H_2 formed could lead to inhibition of the char gasification rate, which is well known [32,36]. The CO also increases simultaneously for the LD slag together with H_2, although the concentration is much lower than the H_2 concentration.

The average char gasification rate between $0.3 < X_c < 0.7$ was found to be almost the same for all bed materials used at lower temperatures, as can be seen in Fig. 6. The time to reach 80% conversion of the char was more similar for olivine and sand, and lower than for the oxygen carriers. A reason why the oxygen carriers have a significantly faster conversion rate of the char at higher temperatures is the higher initial CO_2 release due to the combustion of gasification products with the oxygen carriers, and a considerable difference in the hydrogen concentration, compare to Figs. 3 and 4.

At high temperatures, the gasification rate was two times higher for the oxygen carriers compared to sand and olivine, see Fig. 6. H_2 inhibition could contribute to the significantly slower gasification rate for the two inert materials [34,42]. Here the H_2 maximum partial pressure was about 3 times higher for sand than LD slag and ilmenite, see Fig. 5 for comparison. Even though the cumulative H_2/CO were higher for LD slag than both ilmenite and sand at lower temperature, the same effect could not be observed here. These gasification rates for sand and ilmenite are comparable to earlier studies by Keller et al. [32] where wood char was used in CLC gasification experiments at 970 °C.

3.1.2. Outlet gas composition and WGS

The CO/C_t ratio decreases when oxygen carriers are depleted of oxygen, in comparison to sand, as can be seen in Fig. 7. Although the conversion to CO is the lowest for LD slag, it is quite clear that at lower temperatures the H_2/CO ratio is much higher for LD slag, in comparison to the other studied materials, see Fig. 8.

Fig. 9 shows the total molar production of different gaseous species for the investigated materials given as a fraction of converted fuel in the range of $0.3 < X_c < 0.7$. It can be observed that both oxygen carriers produce less H_2 and CO compared to sand and olivine. Comparing the two oxygen carriers it can be concluded that LD slag produces significantly more H_2 than Ilmenite.

In Fig. 10 the reaction quotient Q_i for the WGS reaction is plotted against the gas char conversion X_c. Here it is clear that the outgoing gases are much closer to the WGS equilibrium (K_{eq}) for LD slag than the other bed materials evaluated in the laboratory fluidized bed. The same trend for LD slag was clear at all different evaluated temperatures. The H_2O concentration was not measured and assumed to be 50%, the same as the ingoing gas composition. Since the concentrations of CO, CO_2 and H_2 in the outgoing gas are much lower than 50%, see Fig. 4 as a comparison, and that the total gasification gas is similar for all samples, this assumption was concluded to be reasonable.

3.1.3. Effects of increased fuel-to-bed ratio

To investigate the effect of increased reduction of the oxygen carrier, more fuel was used to further reduce the bed material, meaning that the fuel-to-bed ratio was increased. The result of a two-fold and three-fold increase in the amount of fuel respectively can be seen in

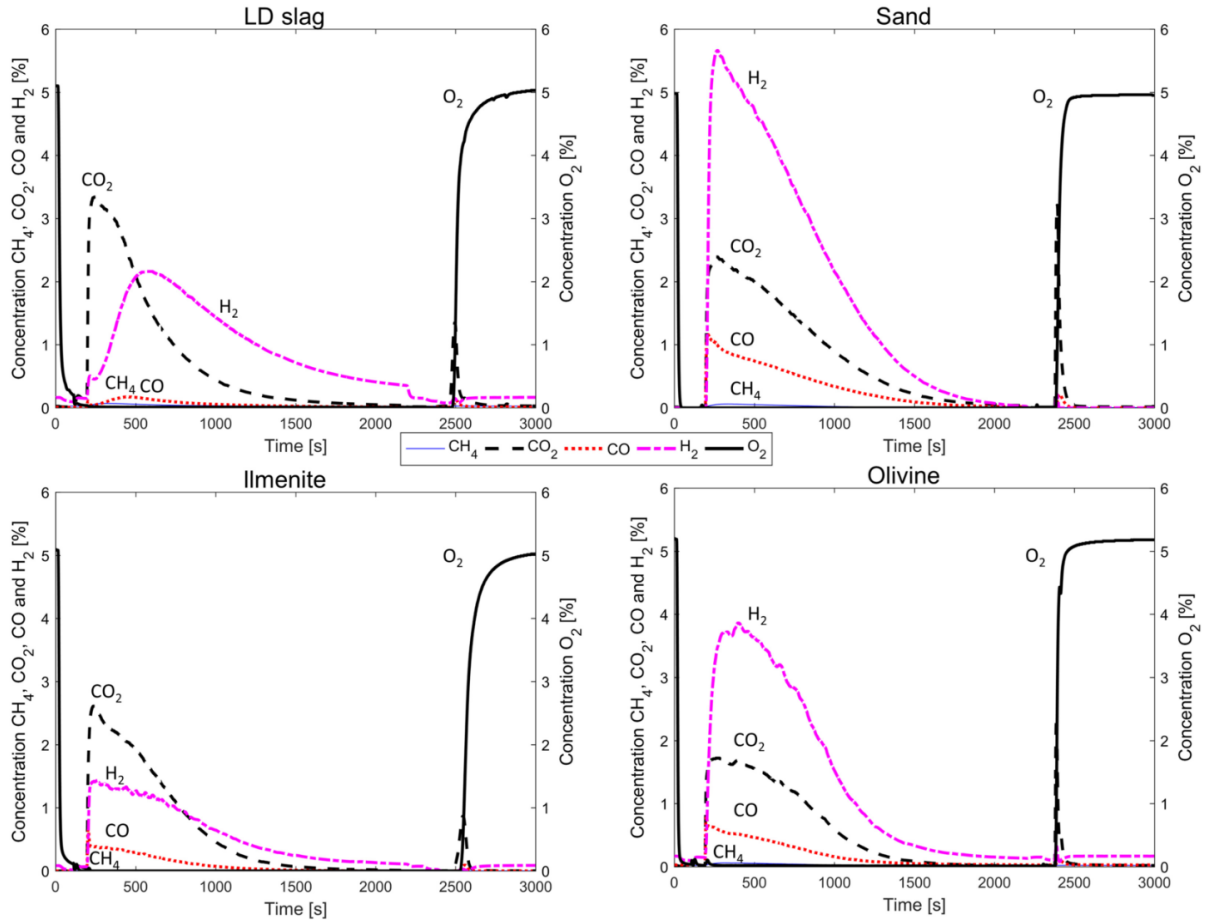

Fig. 4. Raw data plot for the different investigated bed materials during the gasification of biomass char. Cycles displayed here are the third repetition at 870 °C using 0.2 g char. Consult Fig. 3 for information on the different periods (inert/oxidation/fuel addition) in the cycle.

Fig. 11. As could be expected the relative gas to solid fuel generation for H_2 and CO increased as the CO_2 generation decreased. More CO and H_2 compared to CO_2 indicates lower oxygen transport and thus a more concentrated syngas. This is due to the oxygen carrier provides less oxygen per amount of fuel. Comparing ilmenite to LD slag, only a very weak trend towards increased CO generation could be observed for ilmenite by increasing the amount of fuel to reduce the bed more. However, in these experiments, the reduction of ilmenite did not reach the maximum oxygen-carrying capacity.

The overall oxygen transport from the oxygen carrier is also shown in Fig. 11. As it was difficult to accurately calculate the oxygen carrier conversion level during the reduction, here the final conversion level was calculated from the oxidation period following the reduction. It is clear that the degree of oxidation by the oxygen carrier is more or less the same for all LD slag cases independent of the amount of fuel. For the ilmenite cases, there is a continual decrease in the mass-based conversion for all fuel amounts. This indicates that ilmenite still could transport more oxygen even after a three-fold increase in solid fuel addition, while LD slag could not transport more oxygen than it did in the original 0.2 g solid fuel experiment. However, it needs to be acknowledged the strong indications that LD slag is oxidized with steam according to the water-splitting reaction (R5).

In Fig. 12 the gasification rate is displayed for the experiments performed with different amounts of fuel. As could be seen in Fig. 6, the gasification rates for LD slag and ilmenite were very similar when only 0.2 g char was added. However, when increasing the degree of reduction with increased fuel addition, the gasification rate for LD slag is lower compared to ilmenite. It is also very clear that when the generation of H_2 increases for LD slag the gasification rate decreases, as can also be seen in Fig. 5.

3.2. Water splitting

H_2 generation by water splitting could be observed during gasification of solid fuel as seen in Fig. 3 where the H_2 is generated while no CO or CO_2 is produced during the latter parts of the experiment with LD slag. In general, the concentration profiles of H_2 for LD slag during the reduction indicate that water-splitting could also be important when char is present.

Displayed in Fig. 13 are the results of the water-splitting experiments described in Section 2.1.3. From Fig. 13 it is clear that H_2 can be formed during oxidation with H_2O, most likely via the water-splitting reaction given in reaction (R5). However, it was also observed during the oxidation with O_2 that the LD slag absorbed some oxygen. This absorbed oxygen indicates that LD slag was not fully oxidized using only H_2O. This could indicate that LD slag not only transports oxygen by magnetite-wüstite but also, at least partly, is oxidized to a hematite structure or other oxygen-carrying phases not oxidized by steam are active.

3.3. Gaseous fuel experiments

Gaseous fuel experiments were performed to investigate the reactivity of the oxygen carriers with the important gas components CO

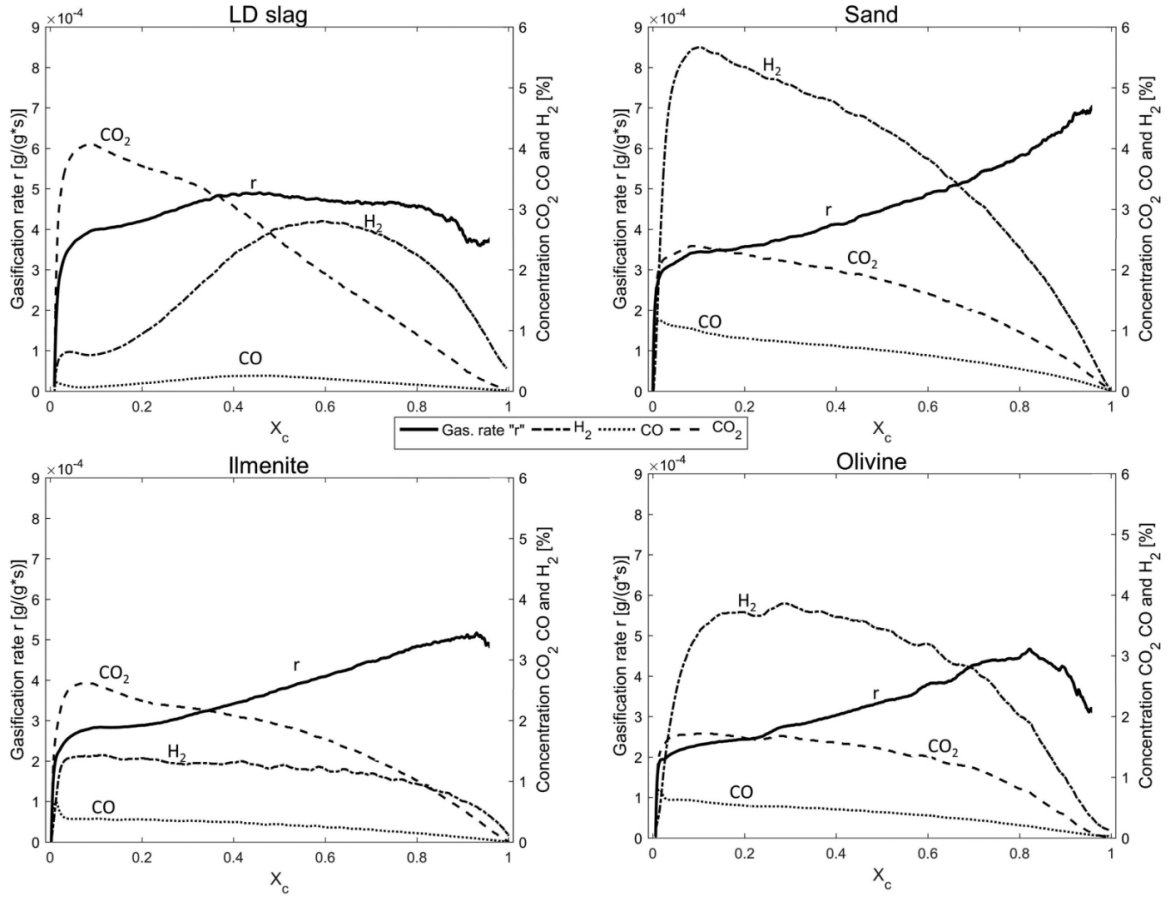

Fig. 5. Gasification rate (r) and concentration of outgoing gases (H_2, CO and CO_2) plotted against the degree of char conversion X_c for investigated bed materials. Data is from a representative cycle at 870 °C for all bed materials using 0.2 g char as a fuel fluidized with 50% steam in N_2.

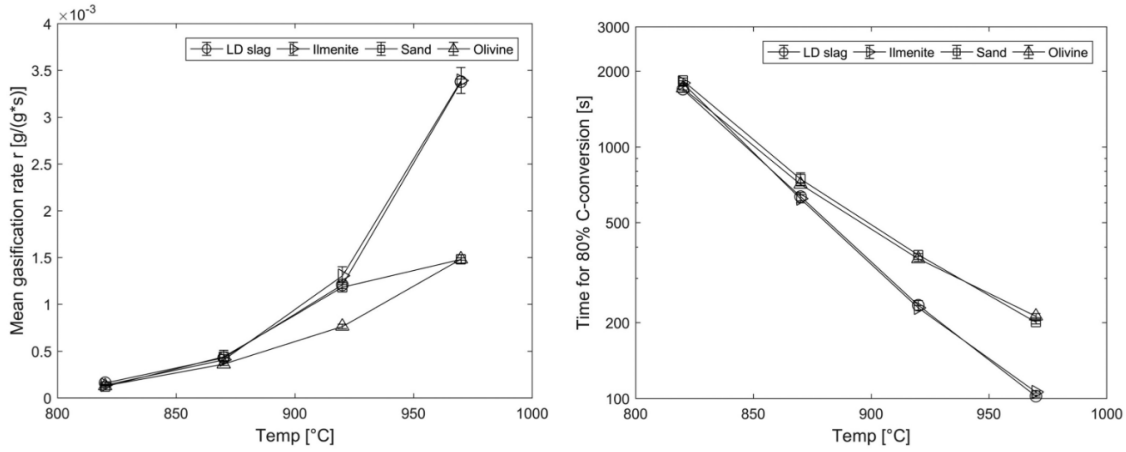

Fig. 6. Left: mean gasification rate (r) for $0.3 < X_c < 0.7$ of the biochar for the investigated bed materials different temperatures using 0.2 g fuel. Right: Time required to convert 80% of the carbon in the biochar to CO, CO_2 and CH_4.

and H_2. This was achieved by exposing the material to both CO and syngas (50% CO, 50%H_2) as described in the experimental section.

Fig. 14 shows the results of the conversion of CO using only CO in N_2 as fuel in the gaseous fuel experiments. Here it is clear that there is an increase in CO conversion with increased temperature. It is also clear that the reactivity of LD slag is decreasing when approaching $\omega = 0.99$ and that the oxygen carrier is reduced below the oxygen-carrying capacity, indicating the formation of most likely elementary iron. In Fig. 15 the results from experiments using CO with and without H_2 are displayed as the conversion of CO (γ_{CO}) at different temperatures and oxidation levels of the oxygen carriers (ω). Clearly, there was a major difference if the pure CO or CO in H_2 was used as fuel. The conversion of CO is considerably lower, especially for LD slag, in the presence of H_2. For ilmenite, the conversion only decreased by roughly 10% but for

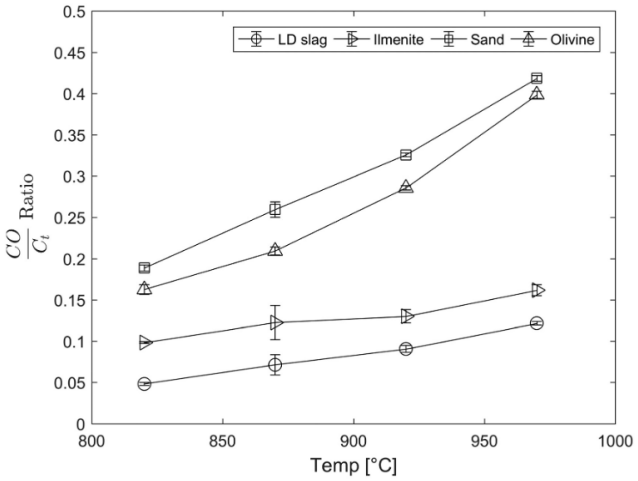

Fig. 7. Fraction of CO to the total emitted carbon during 0.3 < Xc < 0.7 for different temperatures.

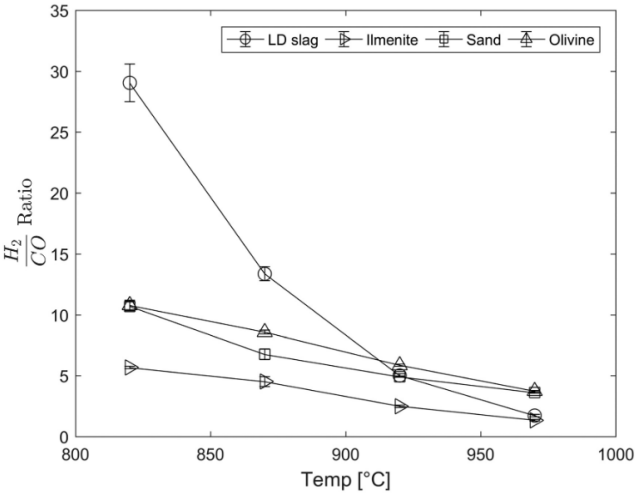

Fig. 8. H_2/CO ratio of outgoing gases at different temperatures for 0.3 < X_c < 0.7.

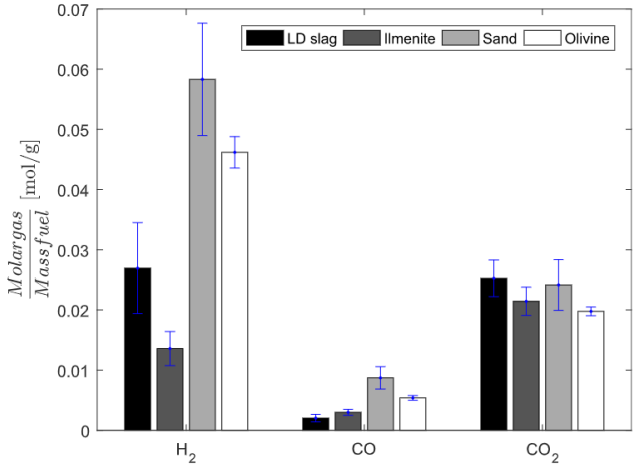

Fig. 9. Molar production of H_2, CO and CO_2 divided by the mass of used solid fuel at 870 °C between 0.3 < X_c < 0.7 for the different bed materials.

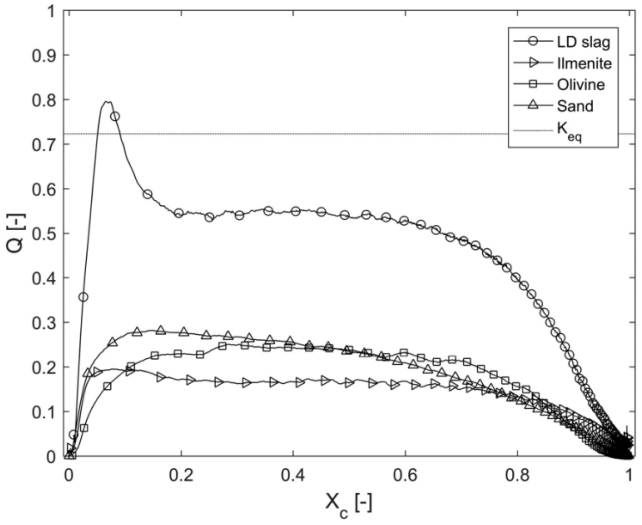

Fig. 10. The reaction quotient (Q_l) related to the WGS reaction for LD slag, ilmenite, olivine and silica sand plotted against the char conversion fraction X_c for one cycle at 870 °C. The plotted cycle is the same as in Fig. 5. The equilibrium constant (K_{eq}) at 870 °C for the WGS reaction is given as a dotted line. Since no H_2O is measured in the outgoing gas the H_2O concentration was assumed to be 50%, same as in the incoming gases to the reactor.

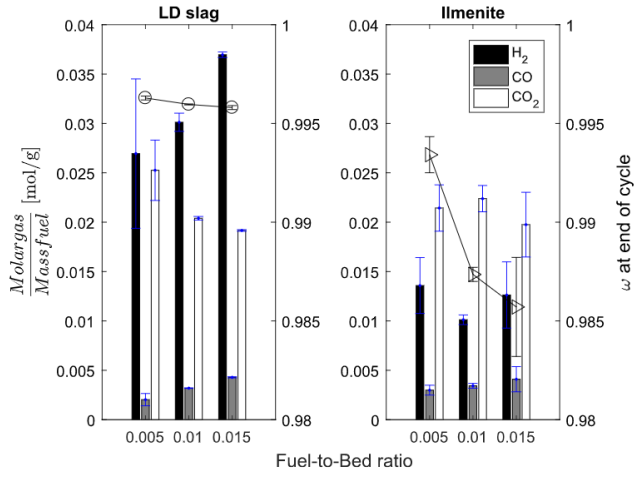

Fig. 11. Molar gas production per gram fuel using LD slag and ilmenite at 870 °C using three different fuel-to-bed ratios. These ratios correspond to a fuel addition of 0.2, 0.4 and 0.6 g respectively to the bed of 40 g oxygen carrier. Calculations on gases are made for 0.3 < X_c < 0.7 to avoid the effect of volatiles. On the right axis is the ω value at the end of the cycle calculated from the absorbed oxygen by re-oxidation.

LD slag, the decrease was more significant, 40–50%. The decrease in γ_{CO} cannot be seen in other experiments where CO and syngas conversion have been compared in a laboratory continuous system using ilmenite [46]. In any case, it is clear that both oxygen carriers are highly reactive towards CO at temperatures relevant for gasification.

The equilibrium constant for the WGS reaction, K_{eq}, varies between 0.65 (970 °C) and 1.8 (670 °C) [43] in the current temperature interval. This means that the reaction is more shifted towards H_2 at low temperatures and more towards CO at high temperatures. This shift, in accordance with WGS, could contribute to the low CO conversion rates at high temperatures and would also explain why LD slag has these features and not ilmenite. This is also in line with the solid fuel experiments where clearly higher H_2/CO ratios are obtained at lower temperatures.

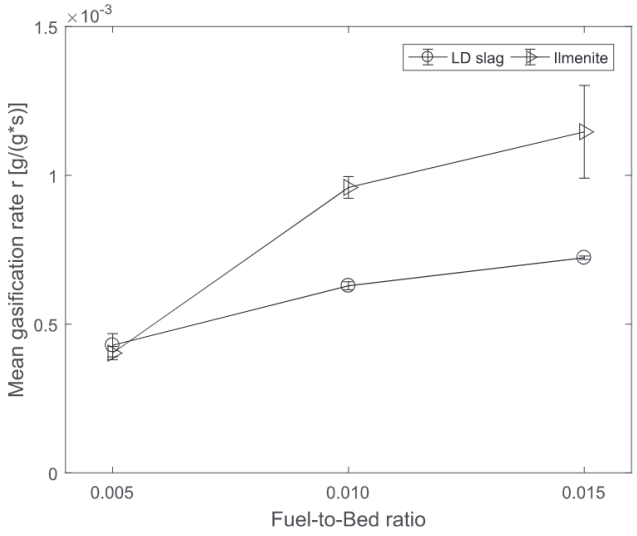

Fig. 12. The mean gasification rate for LD slag and ilmenite with different amounts of fuel-to-bed ratios. These ratios corresponding to a char addition of 0.2, 0.4 and 0.6 g to a bed of 40 g oxygen carrier.

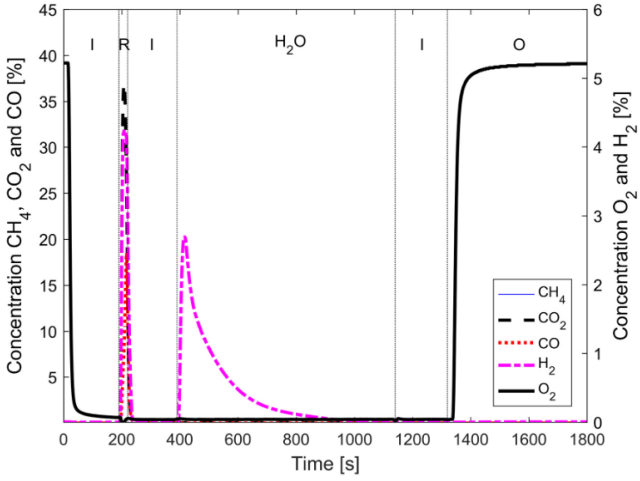

Fig. 13. One cycle of water splitting experiment split up to different phases. 5 g LD slag and 10 g sand were used as bed material and the temperature was set to 870 °C "I" = Inert flush. "R" = reduction with CO. "H_2O" = Oxidation with steam resulting in water splitting and generation of H_2. "O" = Oxidation with 5% O_2.

It was observed in the gaseous fuel experiments at 720 °C and 770 °C for LD slag that a "tail" of CO_2 was present at the end of the reduction phase. Compared to other temperatures and ilmenite experiments the CO_2 concentration decreased slower than the CO concentration after the reduction period. As no char is present at this time, the only source of carbon is likely formed carbonates. However, the CO_2 tail was gone after a few seconds.

3.4. Calcination/carbonation

LD slag contains considerable amounts of free calcium that is converted to CaO at elevated temperatures. The presence of CaO could mean that CO_2 could react with the material forming carbonates. This could affect the gas composition in the fuel reactor, but also mean that CO_2 is released in the air reactor, something which may not be desired if carbon dioxide is to be captured. Results from the calcination/carbonation experiments in the TGA are provided in Fig. 16. Here, the experimental results are compared to the equilibrium of reaction (R7) [47]. The experimental results for LD slag follow the same trend as the equilibrium curve for $CaO/CaCO_3$. However, higher partial pressure of CO_2 is required to form carbonates compared to the equilibrium.

The CO_2 absorption capacity of LD slag was determined to around 1.6 wt%. A slight decrease in the carbonation rate was seen after every cycle for experiments performed with 100% CO_2 at 850 °C. This was expected to be due to structural changes in the particles, but no changes could be visually observed using SEM. The sample could not be investigated further in XRD or by using BET-surface area analysis due to the small amount of sample. However, the same trends towards decreased reaction rate are known from calcium looping where this is known to be a result of sintering and changes in microscopic structure [47]. Still, the important takeaway is that carbonation is possible with this material, which could have implications depending upon operational conditions.

4. Discussion

In this work, a comprehensive study of the feasibility of utilizing LD slag as an oxygen carrier for CLG is presented. It is clear that LD slag's chemical properties affect the gasification process which has been illustrated in a batch fluidized laboratory reactor. It is shown that LD slag not only transfers oxygen through the normal oxygen transfer mechanisms but can also i) catalyze the WGS reaction, ii) react with CO_2 to form carbonates and iii) produce hydrogen through water-splitting.

It was found that LD slag indeed catalyzes the WGS reaction. This is most likely due to the content of CaO in the LD slag. It has been shown in earlier studies that CaO together with an oxygen carrier efficiently catalyzes the WGS reaction [38,48]. WGS was important in the gaseous fuel experiments presented in Fig. 15. Here the CO conversion for LD slag was highly affected by the presence of H_2, compared to ilmenite. This is in contrast to earlier results where lime was added to ilmenite operated with syngas with increasing CO conversion as a result. In that case, it was related to WGS shifting towards increased H_2 and that ilmenite was more reactive towards H_2 than CO, hence increasing the rate of reaction towards H_2 [48]. In this study, LD slag is less reactive towards H_2 compared to CO in contrast to ilmenite. Also, from the gasification experiments in Fig. 10, it is clear that LD slag has catalytic properties that shift the outgoing gases closer to equilibrium compared to the other bed materials. However, it should be noticed that bed materials in a full-scale gasifier likely interacts with ash components, and the surface is thus likely very different than for the particles used in this laboratory reactor. This could have implications, for both the catalyzed reactions as well as char gasification, which can be influenced by, for instance, alkali and calcium depositions [49–51].

It has clearly been shown that the LD slag will react with H_2O via water-splitting forming H_2, according to reaction (R5). This most probably due to the formation of wüstite in these experiments. This occurred both in experiments related to water-splitting in Section 3.2 and during solid fuel gasification experiments where H_2 was generated after no more fuel was converted, see Figs. 3 and 4. The indication that the oxidation to hematite seems to be kinetically hindered, i.e. the oxidation of Fe_3O_4 to Fe_2O_3, means that in principle the water-splitting reaction could be active throughout most of the reduction, although the actual extent is difficult to discern from the current experiments. This is also in alignment with previous XRD results regarding the reduced and oxidized state of activated LD slag [21]. The possibility for water-splitting also suggests that LD slag can be used in CLWS (chemical looping coupled with water splitting).

In this work, WGS and the water-splitting reaction are related to each other. At the same time, these reactions are dependent on the oxygen-carrying potential of the LD slag that converts both H_2 and CO to H_2O and CO_2, respectively as observed in Section 3.3. How these reactions are correlated to each other can also be seen from Fig. 5. It is first after partial char conversion, e.g. when LD slag has been reduced,

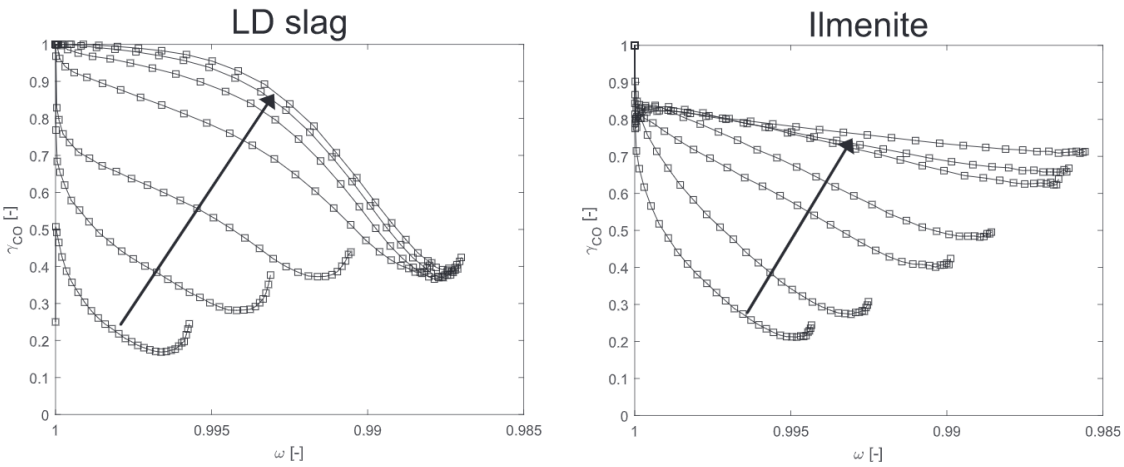

Fig. 14. γ_{CO} plotted against ω for LD slag and ilmenite using 50% CO in N_2 as fuel. Experiments were performed at temperatures from 670 °C to 970 °C, arrow shows the increase of temperature.

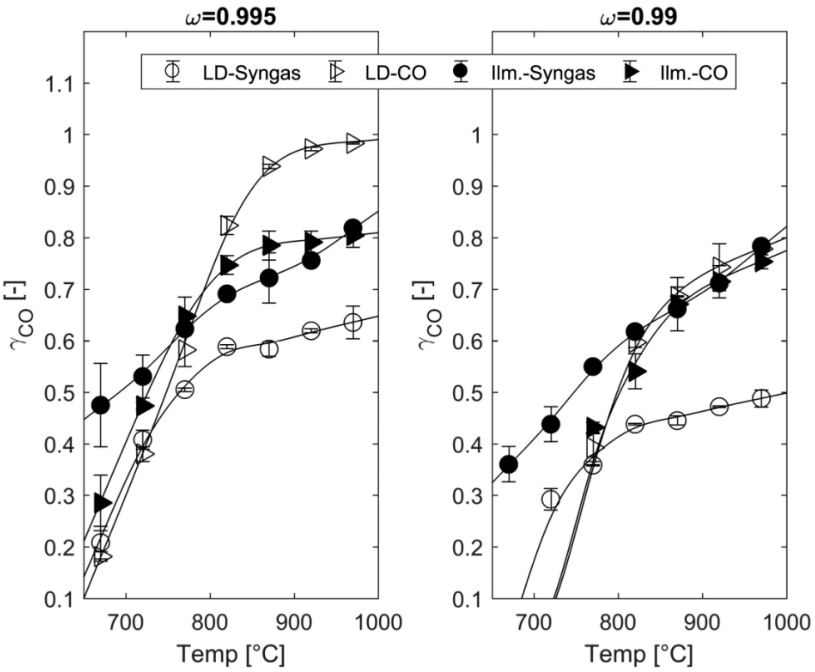

Fig. 15. Plots of partial conversation of CO (γ_{CO}) for syngas (50% CO in H_2) and 50% CO in N_2 for different temperatures at different ω values. The figure to the left is reduced 0.5 wt% compared to the right figure that is reduced by 1 wt%.

that the H_2 concentration increases due to water-splitting. At the same time, the catalyzed WGS reaction shifts the CO_2 towards CO so the reaction quotient Q_i was closer to equilibrium, compare to Fig. 10, and this can be seen as increased CO concentration in Fig. 5. As seen here, it was first after the reduction the H_2 generation from water-splitting was observed as an increase in H_2 concentration. Therefore, by increasing the reduction rate more H_2 should be formed. Also, H_2 generation was increased with an increased fuel-to-bed ratio, see Fig. 11. This could be due that the fuel-to-bed ratio is related to the reduction rate of the bed that promotes the water-splitting reaction. The formed H_2 led to a decreased gasification rate for LD slag compared to ilmenite, see Figs. 11 and 12. This indicates that if high fuel-to-bed ratios are used in a gasifier unit, more H_2 would be generated but to the cost of decreased char conversion rate. Also, since CLG is desired to be operated autothermal, the reduction rate and syngas composition with eventual extra H_2 via water-splitting might be constrained by the heat and oxygen transport control in a continuous process. To comply with the constraints of oxygen transport the bed material must be very reduced in the fuel reactor [7]. In the batch reactor, a more reduced bed was obtained by additional char during gasification. But as could be observed in Figs. 11 and 12 high reduction could not be met and the final measured reduction rate was affected by the water-splitting reaction for LD slag. Never the less, these experiments give an idea of the trend with lower gasification rate of LD slag compared to ilmenite and the impact of water-splitting.

The result of both catalyzed WGS and water-splitting for LD slag is the observed high H_2/CO ratios at temperatures around 820 °C. At the same time, partial combustion due to the presence of an oxygen carrier contribute to the lower CO/C_t ratio, see Figs. 7 and 8. In an ideal process, the lower CO/C_t ratio would not necessarily affect the effective heating value of the outcoming gases in a CLG process. This since the CLG process doesn't require partial combustion of the char in the air

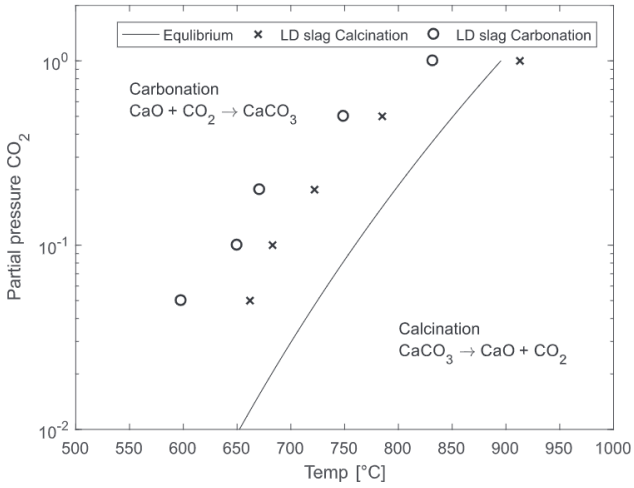

Fig. 16. Equilibrium curve and experimental results of temperature where carbonated LD slag calcine (x) and are carbonatized (o) at a different partial pressure of CO_2. The equilibrium curve is for reaction (R7) and is dependent on both partial pressure CO_2 and temperature.

reactor, see Fig. 1. This is beneficial for CO_2 capture since CO_2 is concentrated into one gas stream, enabling an efficient process for negative emissions with syngas production, provided that biomass is used as fuel [6]. Still, the extent to which oxygen is transported to the fuel reactor is clearly crucial, and it is important to optimize the process in order to avoid combustion of the syngas to a large extent. This may be accomplished in several ways, including adjusting the circulation rate and dilution of the oxygen carriers with an inert material.

The char gasification rate was investigated in this work as well, and it was seen that the rate of char gasification is dependent not only on the extent of the conversion but also by the gaseous environment. H_2-inhibition is one of the reasons why oxygen carriers convert char faster than sand and olivine as can be seen in Fig. 6. However, since LD slag affects the H_2 partial pressure by water-splitting and catalyzed WGS reaction, char is also affected more by H_2-inhibition when using this LD slag as compared to ilmenite. A clear difference between these oxygen carriers can be seen in Fig. 5 where the char conversion rate decreases for LD slag when the H_2 concentration is increased, a behavior that cannot be seen for the other bed materials. Even though the resulting decreased char conversion rate is related to the increasing H_2 concentration, the difference in final char conversion rate for LD slag was limited compared to ilmenite, see Fig. 6.

The char gasification rate was determined to be higher for the oxygen carriers compared to olivine and sand under similar conditions, as can be seen in Fig. 6. Increased temperature resulted in increased gasification rates and higher conversion of H_2 compared to CO, i.e. lower H_2/CO and higher CO/C_t. However, char conversion rates from these experiments may not be possible to extrapolate to a full-scale gasifier. This since the gasification rate is highly affected by activation by alkali and ash [5,16,17,52] that are present in continuous biomass fed gasifier and not in the laboratory batch reactor testing conducted here.

Carbonaton could have a positive effect on the fuel gas composition, as it would remove carbon dioxide from the gas phase, hence promoting H_2 production, see reaction (R7). However, any carbonation will result in carbon being transported as carbonates from the fuel reactor to the air reactor, resulting in decreased CO_2 capture. This phenomenon depends upon the formation of stable carbonates. The carbonate formation, in turn, is depending on i) the partial pressure of CO_2 in the fuel reactor, ii) the temperature and iii) deactivation. As can be seen in Fig. 16, the partial pressure of CO_2 needs to be sufficiently high to be maintained as carbonate and not decompose. At about 870 °C, a partial pressure corresponding to more than 0.8 atm CO_2 is required for calcium carbonate to form if the reactant is CaO according to the same figure. The CO_2 "tail" observed in the syngas experiments was also most likely related to the formation of carbonates. This was only observed for the experiments where a sufficient amount of CO_2 was generated and where the temperature was low enough so that carbonates could be formed. Therefore, it is expected that the transport of carbon as carbonates between the fuel and air reactor will be limited.

This study shows that LD slag can be a promising oxygen carrier for CLG. The combination of reasonable oxygen transport, the possibility for water-splitting and catalysis of the WGS could be advantageous. However, due to the different operating conditions, design of the reactors, presence of ash, bed materials of different origin and alkali activation, the results from the laboratory fluidized bed cannot be directly extrapolated. Still, the results from this work clearly give support to the view that LD slag holds high promise for CLG applications.

5. Conclusion

LD slag, also called steel converter slag, was investigated regarding its effects on gasification of biomass char at CLG condition in a laboratory fluidized batch reactor. Reactions of interest for LD slag investigated in this work were i) oxygen transport and reactivity, ii) catalyzed water-gas-shift reaction, iii) carbonate formation and iv) water-splitting. All these reaction mechanisms can be important depending upon the operating conditions. LD slag was compared to the well-studied oxygen carrier ilmenite as well as conventional sand and olivine as references.

The main findings for LD slag in this work were:

- LD slag successfully transported oxygen to achieve partial oxidation of the gasification products and had a higher gasification rate/char conversion rate compared to sand and olivine.
- LD slag is catalytic towards the water-gas-shift (WGS) reaction.
- When reduced, LD slag reacts with water accordingly to the water-splitting reaction resulting in H_2 generation.
- Both WGS and water-splitting results in a raw gas with high H_2/CO ratios at temperatures around 800 °C when LD slag is used.
- The high H_2 partial pressure results in H_2-inhibition of the char resulting in lower char conversion rate.
- Higher temperatures, 920 °C and above, might increase the CO/C_t ratio but will also result in lower H_2/CO ratios.
- At temperatures above 800 °C, there is no noted absorption of CO_2 due to carbonation. This indicates that carbon will be not transported to the combustor/air reactor as carbonates.

Overall, the low cost and the inherent presence of CaO makes LD slag a good candidate as an oxygen carrier for biomass CLG to achieve a syngas with high H_2/CO ratio and possibilities for generating simultaneous negative emissions.

CRediT statements

Fredrik Hildor: Investigation, Formal analysis, Methodology, Software, Writing - Original Draft, Writing - Review & Editing, Visualization.

Henrik Leion: Writing - Review & Editing, Funding acquisition, Supervision.

Carl Johan Linderholm: Writing - Review & Editing, Supervision.

Tobias Mattisson: Writing - Review & Editing, Funding acquisition, Supervision.

Declaration of competing interest

The authors declare that they have no known competing financial

interests or personal relationships that could have appeared to influence the work reported in this paper.

Acknowledgment

This work was financed by VR, Swedish Research Council (2015-04371) and The Swedish Energy Agency (43220-1). The LD slag bed material was provided by SSAB.

References

[1] C.-Z. Li, Special issue—gasification: a route to clean energy, Process Saf. Environ. Prot. 84 (6) (2006) 407–408.
[2] Z. Min, M. Asadullah, P. Yimsiri, S. Zhang, H. Wu, C.-Z. Li, Catalytic reforming of tar during gasification. Part I. Steam reforming of biomass tar using ilmenite as a catalyst, Fuel 90 (2011) 1847–1854.
[3] V.S. Sikarwar, et al., An overview of advances in biomass gasification, Energy and Environmental Science 9 (10) (Oct. 2016) 2939–2977 (The Royal Society of Chemistry).
[4] J. Koornneef, M. Junginger, A. Faaij, Development of fluidized bed combustion-An overview of trends, performance and cost, Progress in Energy and Combustion Science 33 (1) (Feb. 2007) 19–55 (Pergamon).
[5] H. Thunman, et al., Advanced biofuel production via gasification – lessons learned from 200 man-years of research activity with Chalmers' research gasifier and the GoBiGas demonstration plant, Energy Science and Engineering 6 (1) (Feb. 2018) 6–34.
[6] T. Mattisson, et al., Chemical-looping technologies using circulating fluidized bed systems: status of development, Fuel Process. Technol. 172 (Apr. 2018) 1–12.
[7] A. Larsson, M. Israelsson, F. Lind, M. Seemann, H. Thunman, Using ilmenite to reduce the tar yield in a dual fluidized bed gasification system, Energy and Fuels 28 (4) (2014) 2632–2644.
[8] A. Lyngfelt, A. Brink, Ø. Langørgen, T. Mattisson, M. Rydén, C. Linderholm, 11,000 h of chemical-looping combustion operation—Where are we and where do we want to go? International Journal of Greenhouse Gas Control 88 (2019) 38–56.
[9] T. Mendiara, et al., Negative CO2 emissions through the use of biofuels in chemical looping technology: a review, Applied Energy 232 (2018) 657–684.
[10] H. Leion, T. Mattisson, A. Lyngfelt, Solid fuels in chemical-looping combustion, International Journal of Greenhouse Gas Control 2 (2) (Apr. 2008) 180–193.
[11] H. Leion, T. Mattisson, A. Lyngfelt, Use of ores and industrial products as oxygen carriers in chemical-looping combustion, Energy and Fuels 23 (4) (2009) 2307–2315.
[12] J. Adanez, A. Abad, F. Garcia-Labiano, P. Gayan, L.F. De Diego, Progress in chemical-looping combustion and reforming technologies, Progress in Energy and Combustion Science 38 (2) (Apr. 2012) 215–282.
[13] E. Jerndal, et al., Using low-cost iron-based materials as oxygen carriers for chemical looping combustion chemical looping -an alternative concept for efficient and clean use of Fossil Resources La Boucle Chimique -Un concept alternatif pour un usage propre et efficace des, Oil & Gas Science and Technology – Rev. IFP Energies nouvelles 66 (2) (2011) 235–248.
[14] Ö.F. Dilmaç, N. Dilmaç, E.T. Doruk, Performance of electric arc furnace slag as oxygen carrier in chemical-looping combustion process, Fuel 265 (2020).
[15] J. Marinkovic, H. Thunman, P. Knutsson, M. Seemann, Characteristics of olivine as a bed material in an indirect biomass gasifier, Chem. Eng. J. 279 (Nov. 2015) 555–566.
[16] D. Sutton, B. Kelleher, J.R.H. Ross, Review of literature on catalysts for biomass gasification, Fuel Processing Technology 73 (3) (Nov. 2001) 155–173.
[17] V. Kirubakaran, V. Sivaramakrishnan, R. Nalini, T. Sekar, M. Premalatha, P. Subramanian, A review on gasification of biomass, Renew. Sust. Energ. Rev. 13 (1) (Jan. 2009) 179–186.
[18] T. Berdugo Vilches, M. Seemann, H. Thunman, Influence of in-bed catalysis by ash-coated olivine on tar formation in steam gasification of biomass, Energy and Fuels 32 (9) (2018) 9592–9604.
[19] S. Roudier, L.D. Sancho, R. Remus, M. Aguado-Monsonet, Best Available Techniques (BAT) Reference Document for Iron and Steel Production, (2013).
[20] S. Chand, B. Paul, M. Kumar, Sustainable approaches for LD slag waste management in steel industries: a review, Metallurgist 60 (1–2) (May 2016) 116–128.
[21] F. Hildor, T. Mattisson, H. Leion, C. Linderholm, M. Rydén, Steel converter slag as an oxygen carrier in a 12 MWth CFB boiler – ash interaction and material evolution, International Journal of Greenhouse Gas Control 88 (Sep. 2019) 321–331.
[22] M. Rydén, M. Hanning, F. Lind, Oxygen carrier aided combustion (OCAC) of wood chips in a 12 MWth circulating fluidized bed boiler using steel converter slag as bed material, Applied Sciences 8 (12) (Dec. 2018) 2657.
[23] P. Moldenhauer, C. Linderholm, M. Rydén, A. Lyngfelt, Avoiding CO_2 capture effort and cost for negative CO_2 emissions using industrial waste in chemical-looping combustion/gasification of biomass, Mitigation and Adaptation Strategies for Global Change 25 (1) (2019) 1–24.
[24] J. Waligora, D. Bulteel, P. Degrugilliers, D. Damidot, J.L. Potdevin, M. Measson, Chemical and mineralogical characterizations of LD converter steel slags: a multi-analytical techniques approach, Mater. Charact. 61 (1) (Jan. 2010) 39–48.
[25] M. Keller, H. Leion, T. Mattisson, H. Thunman, Investigation of Natural and Synthetic Bed Materials for Their Utilization in Chemical Looping Reforming for Tar Elimination in Biomass-Derived Gasification Gas, (2014).
[26] L. Xu, G.L. Schwebel, P. Knutsson, H. Leion, Z. Li, N. Cai, Performance of industrial residues as low cost oxygen carriers, Energy Procedia 114 (Jul. 2017) 361–370.
[27] T. Mattison, F. Hildor, Y. Li, C. Linderholm, Negative Emissions of Carbon Dioxide Through Chemical-Looping Combustion (CLC) and Gasification (CLG) Using Oxygen Carriers Based on Manganese and Iron, (2019).
[28] F. Eliasson Störner, F. Hildor, H. Leion, M. Zevenhoven, L. Hupa, M. Rydén, Potassium ash interactions with oxygen carriers steel converter slag and iron mill scale in Chemical-Looping Combustion of biomass – experimental evaluation using model compounds, Energy & Fuels 34 (2) (2020) 2304–2314.
[29] J. Wu, et al., Chemical looping gasification of lignin with bimetallic oxygen carriers, International Journal of Greenhouse Gas Control 93 (2020).
[30] Y. Wang, P. Niu, H. Zhao, Chemical looping gasification of coal using calcium ferrites as oxygen carrier, Fuel Process. Technol. 192 (Sep. 2019) 75–86.
[31] J. Corella, M.P. Aznar, J. Delgado, M.P. Martinez, J.L. Aragües, The deactivation of tar cracking stones (dolomites, calcites, magnesites) and of commercial methane steam reforming catalysts in the upgrading of the exit gas from steam fluidized bed gasifiers of biomass and organic wastes, Stud. Surf. Sci. Catal. 68 (C) (Jan. 1991) 249–252.
[32] M. Keller, H. Leion, T. Mattisson, A. Lyngfelt, Gasification inhibition in chemical-looping combustion with solid fuels, Combustion and Flame 158 (3) (Mar. 2011) 393–400.
[33] B. Bayarsaikhan, et al., Inhibition of steam gasification of char by volatiles in a fluidized bed under continuous feeding of a brown coal, Fuel 85 (3) (2006) 340–349.
[34] C. Fushimi, T. Wada, A. Tsutsumi, Inhibition of steam gasification of biomass char by hydrogen and tar, Biomass Bioenergy 35 (1) (Jan. 2011) 179–185.
[35] B.G. Miller, D.A. Tillman, Combustion Engineering Issues for Solid Fuel Systems, (2008).
[36] K.J. Hüttinger, W.F. Merdes, The carbon-steam reaction at elevated pressure: formations of product gases and hydrogen inhibitions, Carbon 30 (6) (1992) 883–894.
[37] M. Rydén, M. Arjmand, Continuous hydrogen production via the steam-iron reaction by chemical looping in a circulating fluidized-bed reactor, Int. J. Hydrog. Energy 37 (6) (Mar. 2012) 4843–4854.
[38] G.L. Schwebel, H. Leion, W. Krumm, Comparison of natural ilmenites as oxygen carriers in chemical-looping combustion and influence of water gas shift reaction on gas composition, Chem. Eng. Res. Des. 90 (9) (Sep. 2012) 1351–1360.
[39] A. Corcoran, J. Marinkovic, F. Lind, H. Thunman, P. Knutsson, M. Seemann, Ash properties of ilmenite used as bed material for combustion of biomass in a circulating fluidized bed boiler, Energy and Fuels 28 (12) (Dec. 2014) 7672–7679.
[40] H. Thunman, F. Lind, C. Breitholtz, N. Berguerand, M. Seemann, Using an oxygen-carrier as bed material for combustion of biomass in a 12-MWth circulating fluidized-bed boiler, Fuel 113 (Nov. 2013) 300–309.
[41] H. Leion, V. Frick, F. Hildor, Experimental method and setup for laboratory fluidized bed reactor testing, Energies 11 (10) (2018) 2505.
[42] G. Azimi, M. Keller, A. Mehdipoor, H. Leion, Experimental evaluation and modeling of steam gasification and hydrogen inhibition in Chemical-Looping Combustion with solid fuel, International Journal of Greenhouse Gas Control 11 (Nov. 2012) 1–10.
[43] J.M. Moe, Design of water-gas shift reactors, Chem. Eng. Prog. 58 (1962) 33–36.
[44] F. Bustamante, et al., High-temperature kinetics of the homogeneous reverse water-gas shift reaction, AICHE J. 50 (5) (May 2004) 1028–1041.
[45] S. Sundqvist, M. Arjmand, T. Mattisson, M. Rydén, A. Lyngfelt, Screening of different manganese ores for chemical-looping combustion (CLC) and chemical-looping with oxygen uncoupling (CLOU), International Journal of Greenhouse Gas Control 43 (Dec. 2015) 179–188.
[46] J. Aronsson, E. Krymarys, V. Stenberg, T. Mattisson, A. Lyngfelt, M. Rydén, Improved gas–solids mass transfer in fluidized beds: confined fluidization in chemical-looping combustion, Energy Fuel 33 (5) (May 2019) 4442–4453.
[47] J. Blamey, E.J. Anthony, J. Wang, P.S. Fennell, The calcium looping cycle for large-scale CO2 capture, Prog. Energy Combust. Sci. 36 (2) (Apr. 2010) 260–279.
[48] G. Teyssié, H. Leion, G.L. Schwebel, A. Lyngfelt, T. Mattisson, Influence of lime addition to ilmenite in chemical-looping combustion (CLC) with solid fuels, Energy and Fuels 25 (8) (Aug. 2011) 3843–3853.
[49] M. Kuba, F. Havlik, F. Kirnbauer, H. Hofbauer, Influence of bed material coatings on the water-gas-shift reaction and steam reforming of toluene as tar model compound of biomass gasification, Biomass Bioenergy 89 (Jun. 2015) 40–49.
[50] M. Kuba, F. Kirnbauer, H. Hofbauer, Influence of coated olivine on the conversion of intermediate products from decomposition of biomass tars during gasification, Biomass Conversion and Biorefinery 7 (1) (2017) 11–21.
[51] P. Knutsson, V. Cantatore, M. Seemann, P.L. Tam, I. Panas, Role of potassium in the enhancement of the catalytic activity of calcium oxide towards tar reduction, Appl. Catal. B Environ. 229 (Aug. 2018) 88–95.
[52] T. Berdugo Vilches, J. Marinkovic, M. Seemann, H. Thunman, Comparing active bed materials in a dual fluidized bed biomass gasifier: olivine, bauxite, quartz-sand, and ilmenite, Energy and Fuels 30 (6) (Jun. 2016) 4848–4857 (American Chemical Society).